INVESTIGATION OF THE DYNAMIC RESPONSE OF HYDRAULIC ACTUATOR USING VISION SYSTEM

Dr. Hussam K. Abdul-Ameer* Ali Haddy Nassir ** Dr. Ali I. Mahddi**

Received on:16/11/2008
Accepted on:7/4/2010

Abstract

In this research, the dynamic response of the electro-hydraulic system was investigated and analyzed based on a developed vision system. An experimental setup, which consist of hydraulic a circuit (tank, supply pump, pressure gauges, hydraulic actuator, and proportional directional valve) was developed and implemented. In addition, an electronic interface circuit used to control the proportional valve via a personal computer was built. The proposed vision system consists of a digital video camera used to monitor the hydraulic actuator base on two types of camera poses; fixed and on-rod poses. Algorithms and computer programs were implemented for acquiring the image data from the gained video frames. Extra processing steps of the obtained image data were applied to achieve actuator position, velocity, and acceleration. The mathematical model of the developed experimental setup was derived and simulated using SIMULINK software, where it consists of two parts; proportional valve model and hydraulic actuator model.

Evaluation of the theoretical and experimental results and error analyses were presented, where it can be concluded that the use of the vision system as a feedback unit in hydraulic circuit can give promising results in position and force control problem.

استقصاء الاستجابة الديناميكية لذراع هيدروليكي باستخدام منظومة رؤيا

الخلاصة

يهدف البحث الى استقصاء وتحليل الاستجابة الديناميكية لذراع منظومة الكتروهايدروليكية باستخدام منظومة رؤيا(vision system) تتألف من كاميرة فديو رقمية وربط بيني مع الحاسبة الشخصية والتي تعمل كمتحسس لحركة الذراع استعاضة عن المتحسسات التقليدية. حيث تم بناء واعداد منظومة هيدروليكية تتألف من (الخزان , المضخة الدافعة , عدادات لقياس الضغط الهيدروليكي,الذراع الهيدروليكي وصمام تناسبي الكتروهيدروليكي) وكذلك تصميم وتصنيع دائرة الكترونية للسيطرة على الكارت الالكتروني للصمام التناسبي باستخدام الحاسوب الشخصي مما يتيح السيطرة على حركة الذراع الهيدروليكي من خلال الحاسوب وفق الاشارة الداخلة الى الحاسوب.

استخدمت كاميرة فديو رقمية لمراقبة حركة الذراع الهيدروليكي وبوضعيتين الاولى هي الوضعية الثابتة والثانية هي بتثبيت الكاميرا على الذراع الهيدروليكي. طورت خوارزميات لاستخلاص البيانات من سيل الصور (image flow) باعتماد الوضعيتين المقترحتين. تم بناء وبرمجة مجموعة من الخوارزميات لتنقية ومعالجة الصور المكتسبة وتحويلها الى صور ثنائية واجراء معالجة تحديد الحافات وتتبع نقطة على الجسم المتحرك لمعرفة ازاحة , سرعة وتعجيل الذراع الهيدروليكي. تم إعداد نموذج رياضي يحاكي المنظومة الهيدروليكية متمثلا بموديل رياضي لنظام الكتروهيدروليكي يتكون من جزئين , الاول صمام تناسبي كهروهيدروليكي (electrohydraulic proportional valve) والثاني يتمثل في اسطوانة هيدروليكية (hydraulic actuator) , حيث تم بناء برنامج استجابة المنظومة الهيدروليكية باستخدام (SIMULINK).

تضمن البحث اجراء المقارنة والتحليل للنتائج العملية والنظرية وحساب معدل الخطأ والانحراف المعياري للخطأ.

واظهرت النتائج امكانية استخدام منظومة الرؤيا في النظام الهيدروليكي وبصورة واعدة مسقبلا كوحدة تغذية عكسية كجزء من منظومة السيطرة على الموقع والقوة.

*Al-Khwarizmi College of Engineering / Biomedical Eng. Dept. / University of Baghdad
**Al-Khwarizmi College of Engineering / Mechatronics Eng. Dept ./ University of Baghdad

Recently electrohydraulic systems have become increasingly popular in many types of industrial equipment and processes. Such applications include rolling and paper mills, aircrafts, and all kinds of automation in the automobile industry, where linear movements, fast response, and accurate positioning with heavy loads are needed. This is principally due to the high-power density and system solution that they can offer, being less bulky than the DC and AC motors [1].

However, The dynamic performances of hydraulic systems (HS) are highly nonlinear , which complicate the development of high-performance closed loop controllers [2].The nonlinearity of HS is caused by the circuit components of HS, fluid, piping, temperature, and load. For this reason the modeling and control of HS are difficult tasks due to their nonlinear dynamics [3].

One of the improvement techniques tributary to progressing the manufacturing of industry is the addition of the vision-based system to the machine. Vision, in fact, provides a huge amount of information about the environment without any direct physical contact [4]. A basic computer vision system requires a camera, a camera interface, and a computer. In this research, a computer vision system that consists of a digital video camera, camera interface, and a personal computer was used as a feedback sensor to investigate the dynamic response of the HS.

Many researchers studied the field of dynamic response and modeling of HS. In [5], hydraulic control system was developed to achieve automatically adjustment of platform level. A feedback sensor was designed and built based on the variation of the electrical resistance of a photocell that is varying proportionally with the platform level. **Zhao Guojun** [6] developed and analyzed new control strategies for flow control problems in hydraulic elevators, where a control technique using speed feedback was introduced. In [7], a method for modeling an electro–hydraulic system without using the conventional linear models was presented. The Electro-hydraulic components were constructed using the characterization data provided by the manufacturers, and the measurements were obtained in the laboratory with an electrohydraulic manipulator. In [8] ,[9],and [10] they proposed hydraulic control system based on neural network technique. In addition, they presented the mathematical model of the electrohydraulic system based on different assumption.

The main objective of this research is to investigate the dynamic response of the hydraulic actuator when a vision system is used. To achieve the above investigation, an experimental setup consisting of HS and vision system was developed. Also, an electronic circuit that is used as PC-interface with the proportional directional valve is designed and implemented. Algorithms and computer programs are developed to achieve image processing and to extract information from the image scene. The mathematical model of the developed electrohydraulic system,

which consists of the proportional valve and the hydraulic cylinder, is derived and implemented based on previous works.

2. Mathematical Model of HS

The mathematical modeling for both of the proportional valve and the hydraulic cylinder, as shown in figure (1), and hence transfer functions will be derived in this section based on references [10] and [11].

The HS can be separated into two parts, the electrohydraulic valve, which regulates the flow of hydraulic fluid, and the actuation mechanism that generates movement of the joint. The mathematical modeling for both of the proportional directional valve (PDV) and the hydraulic cylinder will be derived in the following subsections.

2.1 The Mathematical Model of (PDV)

The PDA regulates the flow of hydraulic oil by motion of the central spool, which varies the size of the orifice through which the fluid flows. This motion is provided by an electrical solenoid, and the general dynamic analysis of this leads to a fourth-order equation [12].

The total transfer function for the proportional valve is [10]:

$$G_P(S)=\frac{K_m}{(T_s s+1)(T_1 s+1)(T_2 s+1)(T_3 s+1)} \quad (1)$$

Where: T_s is the solenoid time constant.

K_m is the proportional valve gain.

T_1 and T_2 are two time constants of the mechanical system of the PDV.

T_3 is time constant of sliding levers.

Whether zero lap or overlap should be considered. Since the application herein is a position control, then the valve should operate about the neutral point (around zero point in the flow curve, which relates the flow quantity to the rated current used) [11].

Such overlap can be simply modeled by a dead–zone with saturation nonlinearity of 2δ sensitivity bandwidth and of gain K_n ; (as shown in figure(2)). As a result, the output of the proportional valve $f(d)$ is defined as follows:

$$f(d)=\begin{cases}0 & ;|d|<\delta \\ dK_n & ;|d|>\delta\end{cases} \quad (2)$$

2.2 Hydraulic Cylinder Modeling

The hydraulic cylinder can be represented in general by a third order differential equation [13, 14]. However, the nature of this equation (linear or nonlinear) and its coefficients depend on the piston shape and dimensions, fluid properties, pressure used, and sealing performance. In this work a hydraulic cylinder of non-equal piston chambers will be considered.

The model of the hydraulic cylinder can be derived based on the continuity equation and Newtons second law. The

complete derivative of the adopted model is presented in [10].

The specified 3rd-order nonlinear differential equation which governs the piston translation movement (displacement y) have the form :

$$\frac{d^3y}{dt^3}+c_2[c_3c_8+c_7c_4]\frac{d^2y}{dt^2}+c_2[c_6+c_7c_5]\frac{dy}{dt}=c_1c_2f(d) \quad (3)$$

Where:

$$c_1=\frac{1}{2}\frac{K_\mu}{\sqrt{\rho}}[\sqrt{P_s-P_L}+\sqrt{P_s+P_L}]$$

$$c_2=\frac{4\beta A}{m(V_\circ+ay)}$$

$$c_3=\frac{1}{mc_2}=\frac{V_\circ+ay}{4\beta A}$$

$$c_4=\frac{m}{A}$$

$$c_5=\frac{b}{A}$$

$$c_6=A$$

$$c_7=C$$

$$c_8=b$$

- y is the piston displacement (mm).
- m is the total mass of the piston & the load referred to piston (kg).
- b is the viscous damping coefficient of the piston to the load.

Other hydraulic system parameters are described with their units in table (1). In addition, the final numerical values taken to construct the hydraulic system model are listed in the same table, where these values are based on the manufacturing company standard of each part and the experience of expert persons in this field.

As a result, the values of the hydraulic cylinder parameters and *Ci* coefficients can be calculated and their values are listed in table (2).

Figure (3) shows the adopted SIMULINK model of the open loop HS of the developed experimental setup. Where it will be used to obtain the theoretical response of the hydraulic cylinder (displacement, velocity, and acceleration).

3. Experimental Setup

Figure (4) shows a schematic diagram and photographic picture of the developed experimental setup, where it consists of HS (hydraulic pump, proportional valve, hydraulic cylinder, tank, pipes, pressure gauges, DSESEA-card, and developed interface card for controlling the PDV via personal computer) and computer vision system (digital video camera CREATIVE-WEBCAM, interface, and personal computer). Table (3) shows the specification of the experimental setup. Two cameras pose are adopted in this work, fixed and on-rod camera positions. In fixed position, the camera is placed in front of the hydraulic actuator, while in on-rod pose the camera is located on the end of the hydraulic actuator and it is moved when the rod moves. Figure (5) presented a schematic diagram of the adopted camera positions. The complete description of the experimental setup can be seen in reference [15], where the present paper is part of that work.

The response of the hydraulic cylinder (position, velocity, and acceleration) is obtained by using a digital video camera as a position and

velocity sensor. In the following section the image processing techniques that are used to obtain the actuator response based on fixed and on-rod camera poses is described.

4. Image Processing

In this paper, the image flow was acquired using digital video camera type CREATIVE-WEBCAM, where the resolution of the images is digitized at (320×240) pixel with 24 bit color pixels. The adopted frame rate is (5 frame /second). The camera takes the image data and transferrs it to the computer memory using a standard serial link.

Preprocessing algorithms, techniques, and operations are used to perform the initial processing that makes the primary data reduction and analysis task easier. In this paper, the preprocessing step includes four stages where all these stages are done using the simulation blocks of SIMULINK software, figure (6) presented these stages, which are described briefly below.

In the first stage, the image flow is acquired from the used video camera and transferred to SIMULINK as three dimension (3D) array.The obtained array contains color image flow information based on RED,GREEN, and BLUE (RGB) color space model. In the second stage, the 3D array will be converted to gray level array based on PAL equation [16]. The third stage consists of converting the gray level array to the binary array by using the auto-threshold technique that is supported with SIMULINK software. The final stage is the writing of the binary 3D array as a digital video format for further image process and analysis.

After applying the preprocessing stages on the image flow, point tracking algorithm is executed on the obtained binary array to get the dynamic response of the cylinder rod in visual domain, where two algorithms are developed based on the adopted camera poses. The outputs of the developed algorithms are position and velocity of the cylinder rod, while the rod acceleration will be derived based on the rod velocity information.

Since the achieved response of the cylinder rod is in visual domain, a calibration technique is needed to transfer it from visual domain to real world domain. In the following sections, the developed tracking algorithms and calibration methods are presented.

4.1 Fixed-Camera Pose

In this pose, the camera is located in a specific location that allows the camera to monitor the movement of the actuator rod and put it within the field of the view when the camera is capturing the images. As previously illustrated, a calibration process should be done to convert the captured data from the visual scene coordinates (pixel) to real world coordinates (cm).

The developed algorithm is based on tracking a fixed point that is lying on the actuator tip that has a specific location (x,y) at first frame, where this point is chosen to be at the upper-left corner of the rod. When the cylinder

rod is moved, the location of the tracked point is changed in either X or Y direction (depending on the actuator layout) and the new location of the tracked point will be recorded.

The programming steps of the developed algorithm starts by searching the first frame of the binary array about the first black point (belonging to the rod) and recording the (x,y) of the coordinate of the black point. Then, the next frame of the binary array will be processed in the same searching method and so on for other frames. From the recorded coordinates, position and velocity of the cylinder rod can be calculated in visual domain unit (pixel). Figure (7) presents the flowchart of the developed algorithm.

A calibration technique is developed to transfer the obtained response data from visual domain to real world domain based on determining a known specific distance in real world and obtain the perspective distance in visual domain. This method requirs to set the camera in the same place that is used for acquiring the image flow of the cylinder rod. Hence, each 1cm in real world can be converted to the corresponding value of pixels in visual domain and vice versa.

4.2 On-Rod Camera Pose

In this pose, the used camera is placed on the actuator rod, where the camera is moved with the actuator rod and the images are acquired at the same time. The developed algorithm is based on the pre-calibration of a fixed object, which lis in front of the camera. This object has a fixed dimension relative to the monitoring camera. In this work, a circle with 4cm diameter is adopted as a calibration object. The developed algorithm is allowed to track a specific point on the calibration circle in such away when this point is moved in X direction, the respective real displacement in cm of the actuator rod is known. The calibration method in this pose is based on calculating the visual area of the motoring circle at each displacement of the rod.

5. Results and Discussion

The experimental and theoretical results are acquired and studied based on two types of input signals, step and ramp signal. The input signal represents the amount of the input voltage to the DSESAE-CARD which controls PDV and in turn the latter controls the hydraulic cylinder. Six different values of the input voltage are used as step input and one type of signals is used for ramp input. Table (4) shows these input signals and the required time to complete the actuator stroke for both experimental and theoretical conditions.

The results that are gained from the developed experimental setup are processed as described previously, where two camera poses are adopted in this work, fixed and on-rod camera positions. In the following subsections, the results of both camera poses and error calculation are illustrated and discussed.

5.1 Fixed-Camera Pose Results

By observing the general behavior of the result figures (8-13) that are obtained from constant input values of voltage, the unchanging behavior for displacement, velocity, and acceleration of the hydraulic actuator can be explained as follows:

When the amount of input voltage increases, the spool lever moves upward, which causes the increasing of the amount of flow rate to the hydraulic actuator and as a result of that the hydraulic actuator moves due to the applied pressure on the hydraulic piston. By examining the displacement figures (8.a – 13.a), it could be deduced that the required time to accomplish the same amount of the hydraulic actuator displacement at each input is raised. Figures (8.a) and (11.a) shows that the values of the displacement approache to zero value in the first second, this is because of dead-band nonlinearities in the proportional valve which cause this kind of actions.

The velocity responses of all types of step inputs have the same profile, where they increas until they reach a specific point (maximum value) and then decrease in the direction of zero velocity. In addition, it can be seen that the required time that is needed to reach the maximum value of the actuator rod is increased with increasing the input voltage. This response action can be refried to the directional valve design and the length of cylinder stroke.

The acceleration response of the hydraulic actuator for the adopted step inputs are presented in figures (8.c-13.c). The general shape of the acceleration response is linear, where recognized two parts of behavior, can be acceleration (above zero value) and deceleration (under zero value). The acceleration response of hydraulic actuator has a special importance in many applications such as the hydraulic elevator, where it is necessary to control the acceleration with the perfect setting running-curve.

Figure (14) presents the response of the hydraulic actuator for ramp input, where the input voltage to the directional proportional valve is varied from +10V to +15V with step of 1V at each time interval. A different type of behavior can be seen for the actuator velocity (linear rising) because of a continuous increasing of input voltage. The acceleration response performs a linear behavior and it has positive values due to the velocity increasing.

By comparing the experimental and theoretical results for the adopted inputs, it can be seen clearly that both results have approximately identical behavior. However, ripples can be recognized in experimental results because of the following reasons:

The images are captured in an ambient light condition which cause digital noise that can be difficult to remove because the filters may remove the tracking point and this will cause a miss-tracking of the tracked point. In addition, the images are captured at (5 frame/sec) to allow faster response and try to reach real time processing for further control of the process. Because of that, the output curves obtained rippled instead of smooth curved will

be if higher frames per second are picked.

5.2 On-Rod Camera Pose Results

It can be seen from the obtained results, figures(15 – 21), which are based on the developed algorithm for on-rod camera pose, the algorithm succeeds in achieving the theoretical behavior of the position, velocity, and acceleration of the actuator rod. The main advantages of the on-rod camera pose can be illustrate a as follow.

The length of the actuator stroke has no effect on the image acquirement process in contrast with the fixed camera pose, where the increase of the actuator stroke will require replacing of the camera position in the fixed-pose to allow the actuator rod to fall in the field of the view of the monitored camera. The main disadvantage of on-rod pose appears when multi hydraulic cylinders are needed to be monitored. In this case, each cylinder will need a separated vision system to achieve full monitoring of the entire system, while fixed-camera pose will need only single vision system to monitoring the multi cylinder system.

5.3 Error Analysis

In this section, the mean and standard deviation of the errors that are produced between theoretical and experimental results are calculated for the fixed and on-rod camera poses as shown in table (5). The amount of mean error values for different types of inputs lies between 1.7mm to 3.3mm of fixed camera pose and 1.6mm to 5.3 mm of on-rod camera pose. These values show that the fixed pose is more expensive than the on-rod pose, where the main cause of the error is image noises that affect of the performance of the developed algorithm. However, by developing a suitable image filter and more sophisticated tracking algorithm, the error should be decreased in the case of on-rod camera pose than fixed pose because the acquired images will be zoomed in (as camera moved forward) and the obtained image quality will be improved.

The standard deviation value of the different types of inputs is within acceptable range if compared with the respective mean error values in general. These values can give a good indication of the error distribution of each input. In general, the amount of errors show the beneficial results for using vision system as feedback or monitoring unit in hydraulic position control problem.

6. Conclusion

In this paper, the response of the electro-hydraulic system was investigated using a vision system. Results that are obtained from the experimental setup are compared with the simulation results of the mathematical model of the test rig and showed that both results are approximately identical in spite of the ripples that appeared due to light condition, digital noise, fame rate, and non-linearity of the HS.

Both fixed and on-rod camera poses showed acceptable error range, however; the fixed pose was more accurate than on-rod pose. For future work and by using more sophisticated tracking algorithm, it

can be deduced that on-rod pose may be used with confidence as a feedback sensor in HS control problems.

In general, using the vision system in control loop of the HS can be considered as a promising technique.

References

[1] W. Kmmetmüller, S. Müller, and A. Kugi "Mathmatical Modoling and Nonlinear Controller Design for a Novel Electrohydraulic Power-Steering System" IEEE / ASME Trans. On Mechatronics, Vol. 12, No. 1, Feb. 2007, pp. 85-97.
[2] Bin. Yao, "Adaptive Robust Motion Control of Single-Rod Hydraulic Actuators: Theory and Experiments". IEEE / ASME Trans. on Mechatronics, vol. 5, No.1 pp.366-386, 2000.
[3] Carlos L., "Force Tracking Neural Control for an Electro-Hydraulic Actuator via Second Order Sliding Mode". IEEE Journal of Intelligent Control, vol. 10, pp15-30, 2005.
[4] Pitas, I."Parallel Algorithms for Digital Image Processing, Computer Vision and Neural Network," Wiley. , 1995
[5] M. Yhya. "Design and Analysis of Hydraulic Control System for Precise Position". M. Sc. thesis, Mechanical Eng. Dept., University of Baghdad, 1999.
[6] Z. Guojun. "Study on Control Technique of Velocity and Acceleration for Hydraulic Elevator". Ph.D. thesis, Fluid Power Transmission and Control Department, Zhejiang University, 1999.
[7] Zheng D. Li. "Modeling and Simulation of an Electro-Hydraulic Mining Manipulator". Ph.D. thesis, Mechanical Engineering Department, Queensland University, 2000.
[8] Burton R. T. "Neural Network and Hydraulic Control from Simple to Complex Application". Ph.D. thesis, Mechanical Engineering Department, Saskatchewan University, 2001.
[9] Majid A. AL-Faraje. "Theoretical and Experimental Investigation of Proportional Directional Control Valve Performance Using Neural Network". Ph.D. thesis, Mechanical Engineering Department, AL-Mustansiriyah University, 2004.
[10] Eman S. "Neural Network Controller for A Hydraulic System" Ph.D. thesis, Electrical Engineering Department of Technical Education, University of Technology, 2007.
[11] H:Dörr, R. Ewald, F. Liedhegener, J. Hutter, A. Schmih, and D. Kretz. "The Hydraulic Trainer Volume 2–Proportional and Sewo Valve Technology". Mannesmann Rexroth GmbH, 1986.
[12] M.W. Dunnigan, D. M. Lane, A.C. Clegg, and I. Edwards "Hybrid Position/Force Control of a Hydraulic Underwater Manipulator" IEE Proc. Control Theory Appl., Vol. 143, No.2, March 1996.
[13] M. J. Vilenius "The Application of Sensitivity Analysis to Electrohydraulic Position Control Servos" Journal of Dynamic Systems ,Measurement and Control; Vol. 105, pp.77-82, June 1983.
[14] Norvelle F.D., "Electrohydraulic Control Systems", Prentice Hall, 2000.
[15] A. Hadi "A Proposed Vision System with Application to Dynamic Motion of Hydraulic System" M. Sc. thesis, Mechatronics Eng. Dept., Al-Khwarizmi college of Eng., University of Baghdad, 2009.
[16] L. Issa "Vision – Application to Computerized Numerical Control Machine"

M. Sc. thesis, Control and Systems Eng.

Table (1) HS parameters.

Parameters symbol	Description	Value	Unit
K_a	Electrical amplifier gain	26	$mA.v^{-1}$
U_{max}	Maximum voltage to saturation	300	Volt
T_s	Solenoid time constant	2.5×10^{-3}	sec.
K_m	Proportional valve gain	0.04	$mm.A^{-1}$
T_1, T_2	Time constant of mechanical system for the proportional valve	(2.018×10^{-3}) (3.3806×10^{-2})	sec.
T_3	Time constant of sliding lever	8.424×10^{-4}	mm
δ	operating designed value of sliding lever	0.1	mm
δ_d	Mechanical constraints on sliding lever movement	4	mm
K_n	Dead –zone gain	0.2	$mm.v^{-1}$
$V_\circ$	Total fluid volume	264	cm^3
d_1, d_2	Diameters of piston	(60) (36)	mm
P_s	Supply pressure	5.6	M Pa
β	Effective modulus	2.73×10^5	M Pa
ρ	Oil density	-	$kg.m^{-3}$
$\frac{K_m}{\sqrt{\rho}}$	-	2.57×10^{-4}	$m^2.sec^{-1}.Pa^{-0.5}$
m	Total mass of piston &load referred to piston	3	kg
b	Viscous damping coefficient	1.66×10^6	$N.sec.m^{-1}$

Table (2) values of hydraulic cylinder parameters and *Ci* coefficients.

Parameters &coefficients	Values and units	Parameters &coefficients	Values and units
A_1	$28.27 cm^2$	c_3	$4.48\times10^{-8}+6.64\times10^{-9}\,y$
A_2	$18\ cm^2$	$\bar{c}_3$	$4.1\times10^{-7}\ cm^3.\mathrm{N}^{-1}$
A	$23\ cm^2$	c_4	$0.13\ \mathrm{K}g.cm^{-2}$
a	$10\ cm^2$	c_5	$515.5\ \mathrm{N.sec}.cm^3$
P_L	$64.2\ \mathrm{MP}a$	c_6	$23\ cm^2$
c_1	$8500\ cm^2.\mathrm{sec}^{-1}$	c_7	$0.01\ cm^3.\mathrm{sec}^{-1}.\mathrm{P}a^{-1}$
c_2	$5.22\times1^6(69.5+10.3y)$	c_8	$1.66\times10^4\ \mathrm{N.sec}.cm^{-1}$
$\bar{c}_2$	$2289\ cm^{-2}.\mathrm{sec}^{-2}$		

Table (3) Experimental Setup specifications.

Part #	Part Name	Specification
1	Hydraulic Pump	REXROTH / Switzerland HLA 197
2	Hydraulic Cylinder	REXROTH (single- rod/double acting) *355256/9* No 4927 F08
3	PDV	REXROTH/ W. Germany 4 WRE 6E08-11 / 24Z4 / M RN 176.91 Blatt 1 H
4	DSCSEA-CARD Dual Stroke Controlled Solenoid Electronic Amplifier	REXROTH/ W. Germany Prop. Amplifier 11110086 VT5005 S13 R5 engl. 211879/16
5	PC-Interface Card	Developed by the researcher (Parallel port)
6	Digital Camera	CREATIVE-WEBCAM / RGB 24bit / 320×240 Res.

Table (4) Theoretical and Experimental Conditions.

Type of input	Experimental		Theoretical	Time(sec)
	Supply voltage(v)	I/P signal	Signal input(voltage)	
Step1	0.75	15	0.1	8.2
Step2	1.38	14	1.2	13.4
Step3	2.2	13	2.3	18.2
Step4	3.15	12	3.4	18.8
Step5	3.8	11	4.4	20.2
Step6	4.77	10	5.5	25.4
Ramp	0.75-4.77	10-15	0.1-5.5	12

Table (5) Mean and standard deviation of position error.

Case no.	Fixed camera (mm)		On-Rod camera (mm)	
	Mean error	Standard deviation	Mean error	Standard deviation
Step1	1.8248	1.0261	3.4327	2.4312
Step2	1.9611	1.2712	1.6921	1.3156
Step3	1.7702	1.2342	3.7768	2.3275
Step4	2.4663	1.5450	4.3504	2.5856
Step5	2.6580	1.6263	5. 1696	2.6219
Step6	3.3373	2.4852	5.2673	2.7459
Ramp	2.8078	1.9510	3.0736	1.7361

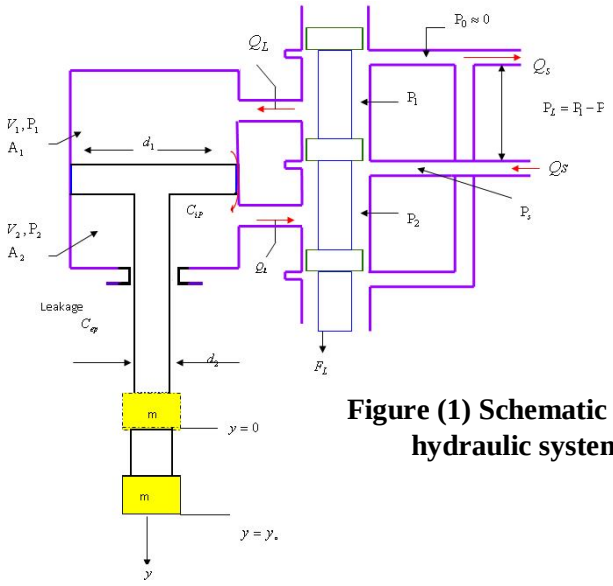

Figure (1) Schematic diagram of hydraulic system [10].

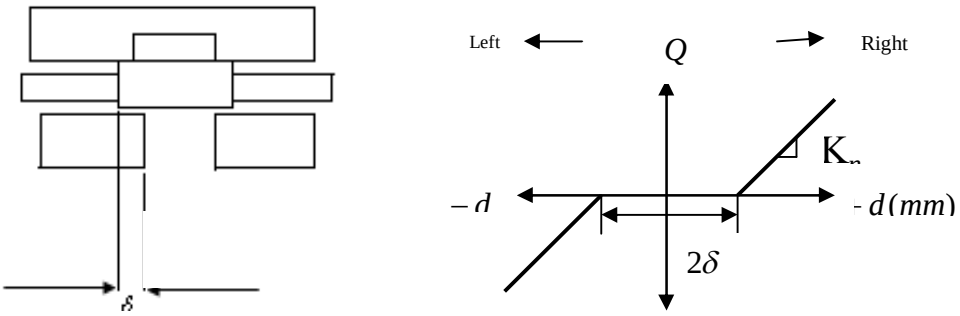

Figure (2) Overlap model [10].

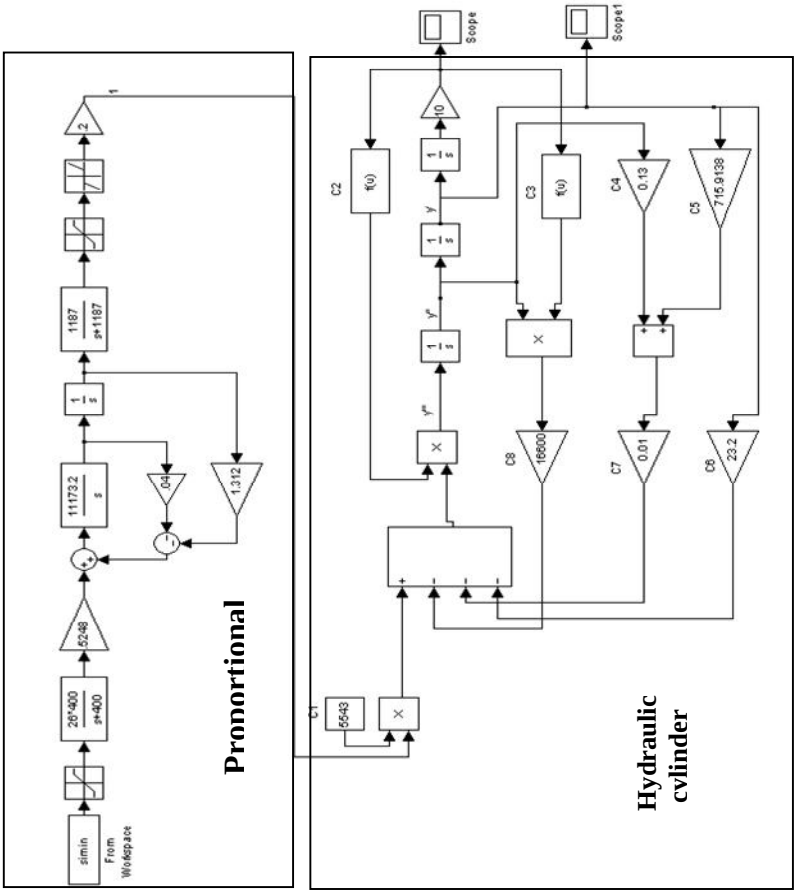

Figure (3) SIMULINK model of the adopted HS.

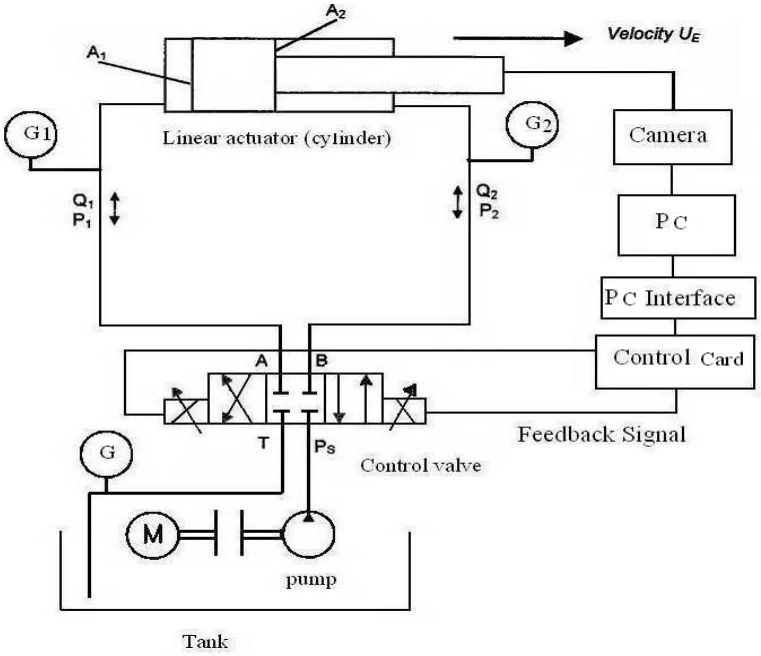

(A) Schematic diagram of the developed experimental setup.

(B) photograph of the developed system.

Figure (4) Experimental setup.

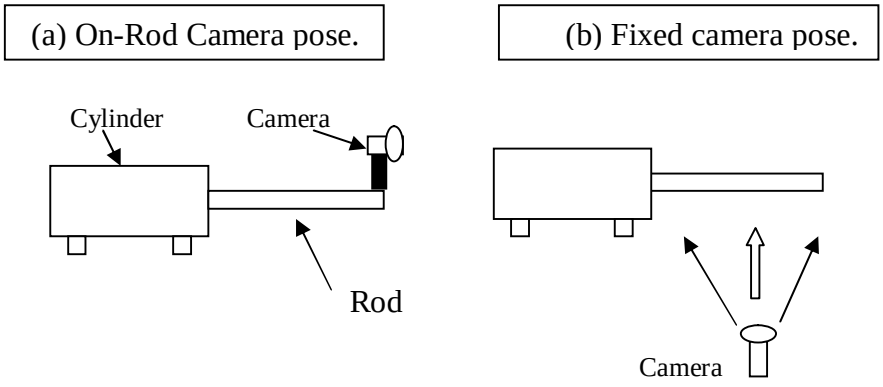

Figure (5) Schematic diagram of the adopted

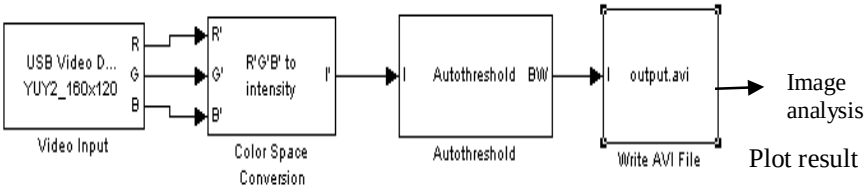

Figure (6) SIMULINK Blocks of image acquisition and preprocessing.

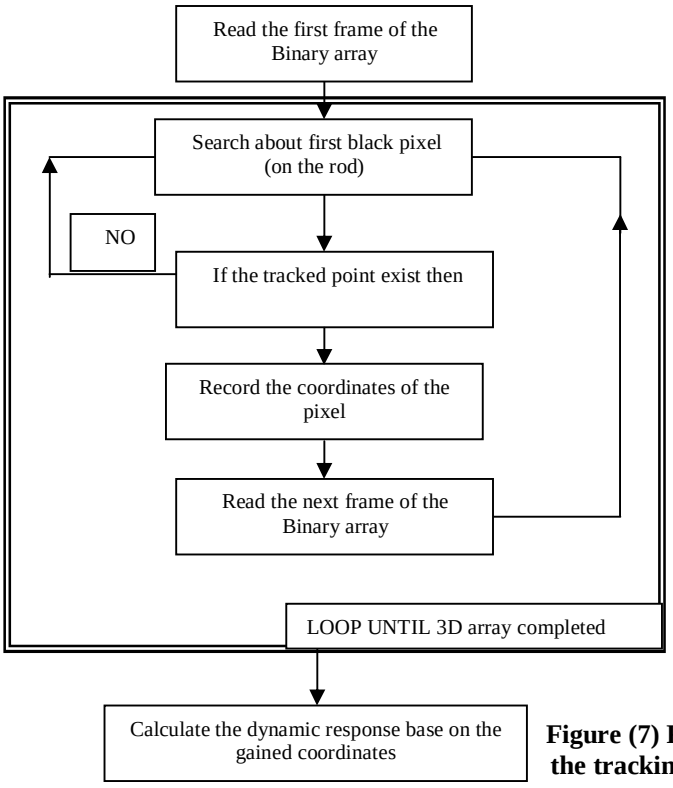

Figure (7) Flowchart of the tracking algorithm.

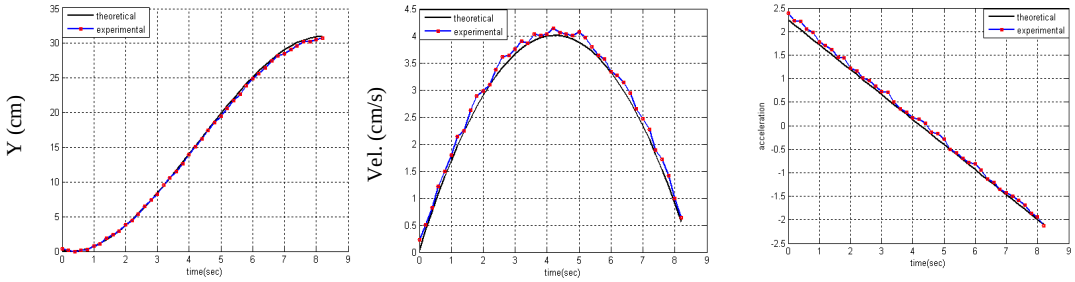

a. Theoretical and experimental displacement of the actuator of step1 input

b. Theoretical and experimental velocity of the actuator of step1 input

c. Theoretical and experimental acceleration of the actuator of step1

Figure (8) fixed camera position results of step1

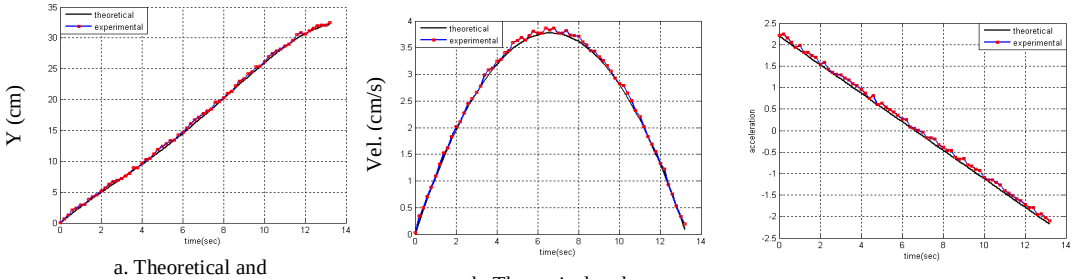

a. Theoretical and experimental displacement of the actuator of step2

b. Theoretical and experimental velocity of the actuator of step2 input

c. Theoretical and experimental acceleration of the actuator of step2 input

Figure (9) fixed camera position results of step2

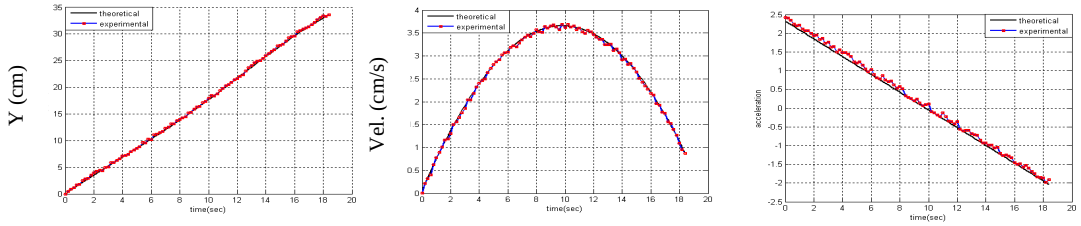

a. Theoretical and experimental displacement of the actuator of step3 input

b. Theoretical and experimental velocity of the actuator of step3 input

c. Theoretical and experimental acceleration of the actuator of step3 input

Figure (10) fixed camera position results of step3

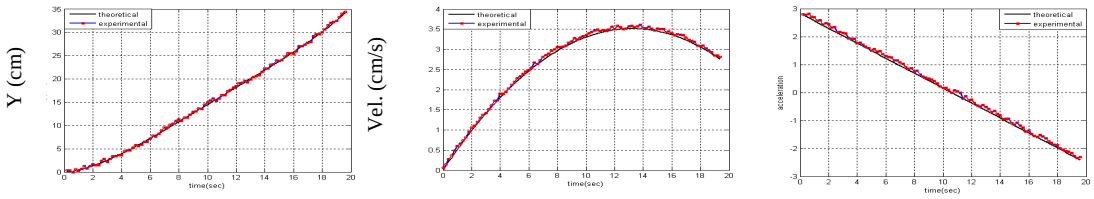

a. Theoretical and experimental displacement of the actuator of step4 input

b. Theoretical and experimental velocity of the actuator of step4 input

c. Theoretical and experimental acceleration of the actuator of step4

Figure (11) Fixed camera position results of step4.

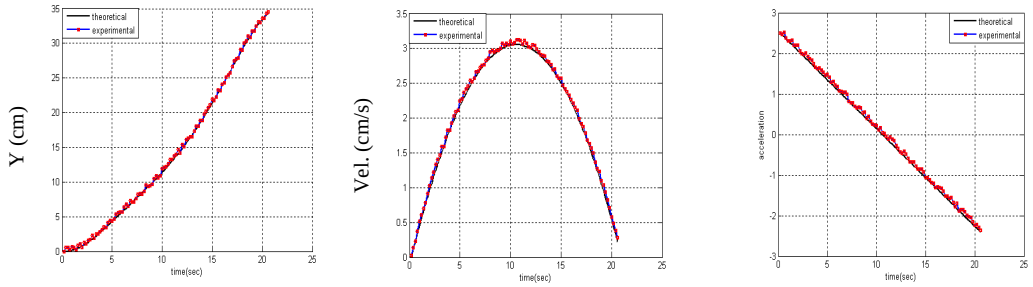

a. Theoretical and experimental displacement of the actuator of step5 input

b. Theoretical and experimental velocity of the actuator of step5 input

c. Theoretical and experimental acceleration of the actuator of step5 input

Figure (12) Fixed camera position results of step5

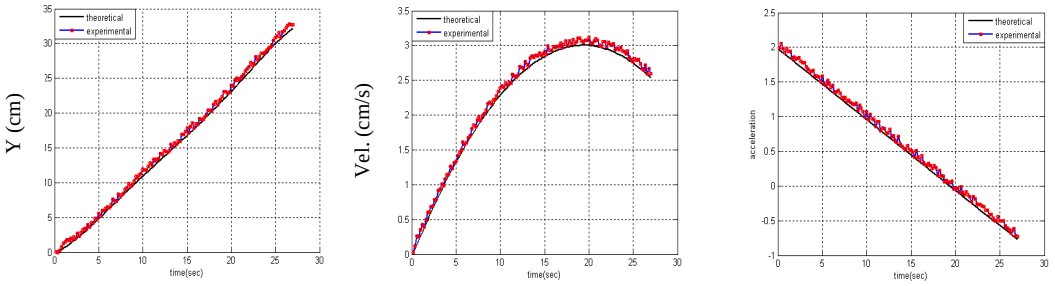

a. Theoretical and experimental displacement of the actuator of step6 input

b. Theoretical and experimental velocity of the actuator of step6 input

c. Theoretical and experimental acceleration of the actuator of step6 input

Figure (13) Fixed camera position results of step6

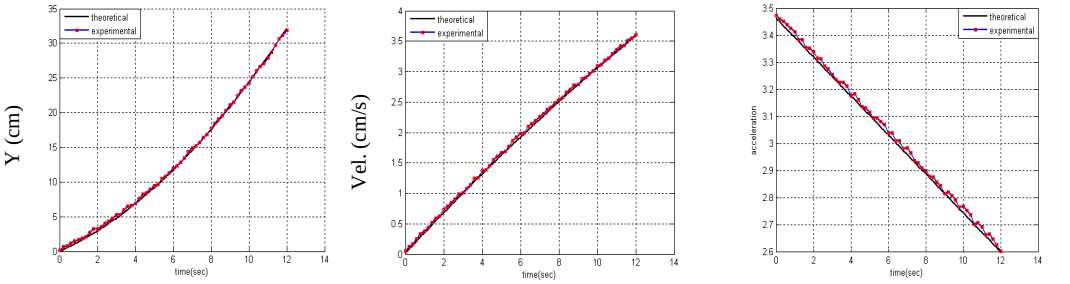

a. Theoretical and experimental displacement of the actuator of ramp input

b. Theoretical and experimental velocity of the actuator of ramp input

c. Theoretical and experimental acceleration of the actuator of ramp input

Figure (14) Fixed camera position results of ramp

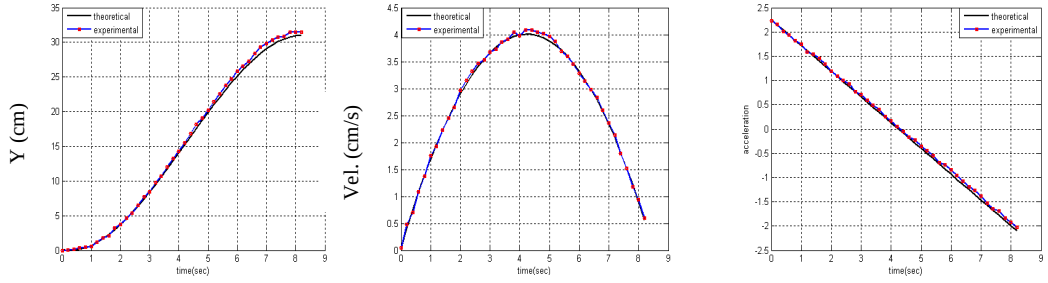

a. Theoretical and experimental displacement of the actuator of step1 input

b. Theoretical and experimental velocity of the actuator of step1 input

c. Theoretical and experimental acceleration of the actuator of step1 input

Figure (15) on-rod camera position results of step1

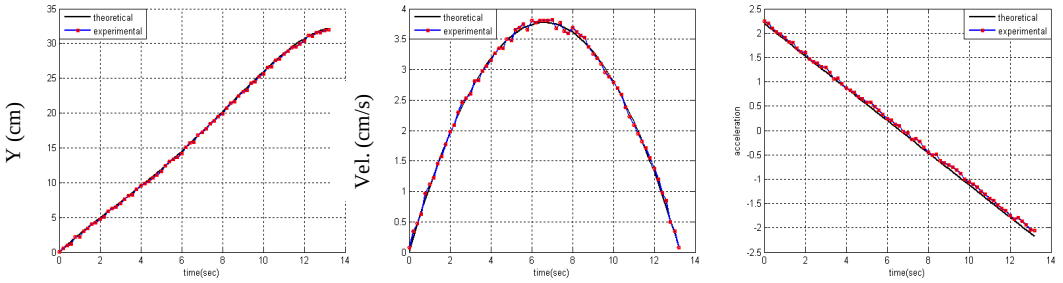

a. Theoretical and experimental displacement of the actuator of step2 input

b. Theoretical and experimental velocity of the actuator of step2 input

c. Theoretical and experimental acceleration of the actuator of step2 input

Figure (16) on-rod camera position results of step2

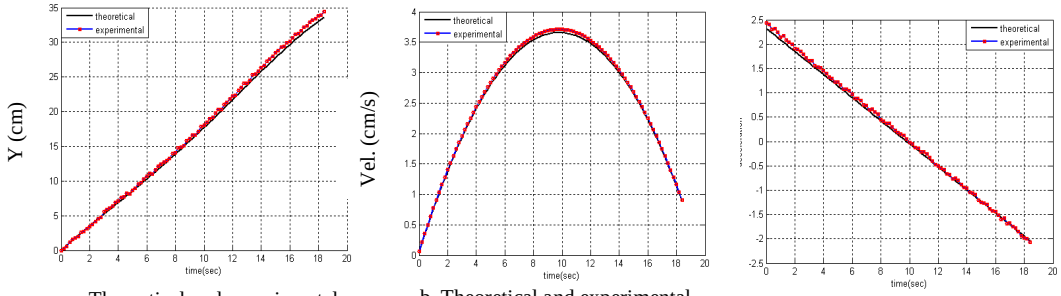

a. Theoretical and experimental displacement of the actuator of step3 input

b. Theoretical and experimental velocity of the actuator of step3 input

c. Theoretical and experimental acceleration of the actuator of step3 input

Figure (17) on-rod camera position results of step3

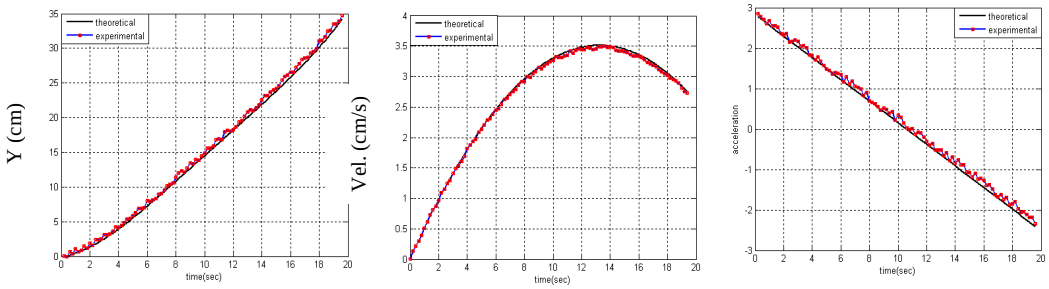

a. Theoretical and experimental displacement of the actuator of step4 input

b. Theoretical and experimental velocity of the actuator of step4 input

c. Theoretical and experimental acceleration of the actuator of step4 input

Figure (18) on-rod camera position results of step4

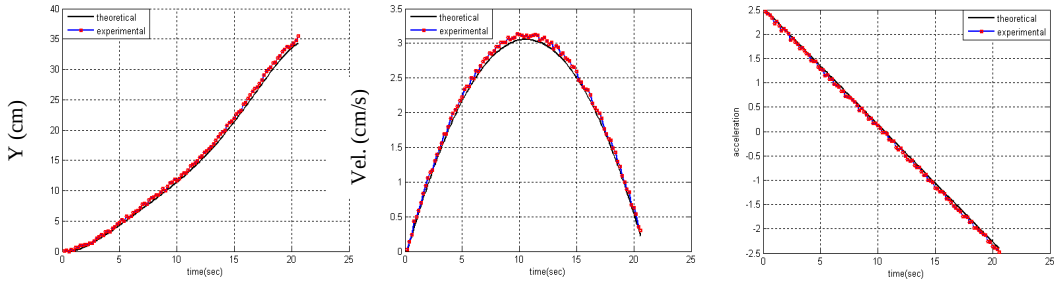

a. Theoretical and experimental displacement of the actuator of step5 input

b. Theoretical and experimental velocity of the actuator of step5 input

c. Theoretical and experimental acceleration of the actuator of step5 input

Figure (19) on-rod camera position results of step5

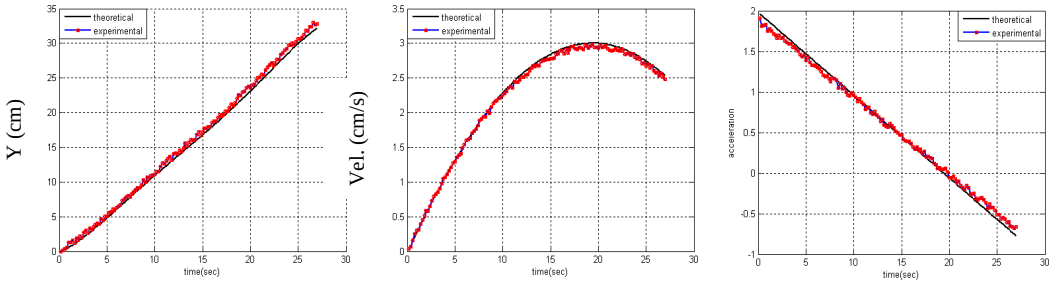

a. Theoretical and experimental displacement of the actuator of step6 input

b. Theoretical and experimental velocity of the actuator of step6 input

c. Theoretical and experimental ıcceleration of the actuator of step6 input

Figure (20) on-rod camera position results of step6

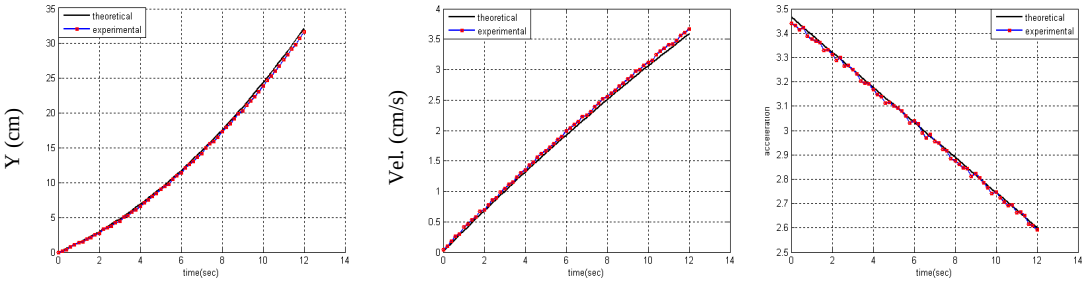

a. Theoretical and experimental displacement of the actuator of ramp input

b. Theoretical and experimental velocity of the actuator of ramp input

c. Theoretical and experimental acceleration of the actuator of ramp input

Figure (21) on-rod camera position results of ramp